

Article

Design Evaluation and Performance Analysis of a Double-Row Pneumatic Precision Metering Device for *Brassica chinensis*

Bohong Li^{1,2}, Riaz Ahmad^{2,3}, Xindan Qi^{1,*}, Hua Li^{2,3,*}, Samuel Mbugua Nyambura^{2,3} , Jufei Wang^{2,3}, Xi Chen^{1,2} and Shengbing Li^{1,2}

¹ College of Mechanical and Power Engineering, Nanjing Tech University, Nanjing 211816, China; li_bohong319@163.com (B.L.); njut_chenxi@163.com (X.C.); lishengbing1996@163.com (S.L.)

² Key Laboratory of Intelligent Agricultural Equipment in Jiangsu Province, Nanjing Agricultural University, Nanjing 210031, China; Riazahmad@njau.edu.cn (R.A.); accessmbugua@gmail.com (S.M.N.); wangjufei@stu.njau.edu.cn (J.W.)

³ College of Engineering, Nanjing Agricultural University, Nanjing 210031, China

* Correspondence: xindanqi@njtech.edu.cn (X.Q.); lihua@njau.edu.cn (H.L.)

Abstract: In view of the low seeding efficiency and precision of seeders used for *Brassica chinensis* in China, a new double-row pneumatic precision metering device for *Brassica chinensis* was designed, fabricated, and evaluated. With the characteristics of small size and high sphericity of *Brassica chinensis* seeds in mind, the structure and key dimensions of the metering plate were determined, and a force analysis of the seed-filling process was carried out. The negative pressure (NP), angular velocity (AV) of the metering plate, and cone angle (CA) of the suction hole were selected as the main influencing factors of the experiment. In order to explore the influence of each single factor and the interaction between factors on the seeding performance, a single factor experiment and a central composite design (CCD) experiment were designed, respectively, and the experimental results were analyzed by analysis of variance (ANOVA). After optimizing the main influencing factors such that the target of the qualified index (QI) was greater than 94% and the miss index (MI) was less than 2.5%, it was found that when CA was 60°, NP was 1.55–1.72 kPa, and AV was 1.1–1.9 rad/s, the seeding performance was excellent. The bench verification results of seeding performance (94% ≤ Q ≤ 100%, 0 ≤ M ≤ 2.5%) and the coefficient of variation (CV) of seed mass (CV of seed mass in outer and inner circle: 5.15%; CV of total seed mass: 8.60%) under the condition of parameter optimization were analyzed; as a result, the accuracy of the parameter optimization was confirmed.

Keywords: ANOVA; *Brassica chinensis*; coefficient of variation; double-row; metering device; pneumatic



Citation: Li, B.; Ahmad, R.; Qi, X.; Li, H.; Nyambura, S.M.; Wang, J.; Chen, X.; Li, S. Design Evaluation and Performance Analysis of a Double-Row Pneumatic Precision Metering Device for *Brassica chinensis*. *Sustainability* **2021**, *13*, 1374. <https://doi.org/10.3390/su13031374>

Academic Editor: Muhammad Sultan

Received: 10 December 2020

Accepted: 12 January 2021

Published: 28 January 2021

Publisher's Note: MDPI stays neutral with regard to jurisdictional claims in published maps and institutional affiliations.



Copyright: © 2021 by the authors. Licensee MDPI, Basel, Switzerland. This article is an open access article distributed under the terms and conditions of the Creative Commons Attribution (CC BY) license (<https://creativecommons.org/licenses/by/4.0/>).

1. Introduction

Brassica chinensis (BC) is rich in vitamins and minerals, with a high plant cellulose content. It is widely cultivated in China because its vegetable is favored by people in the North and South [1]. The planting mode of BC is mainly individual planting in China, and artificial seeding is also the main method for the plantation process. Because this kind of seeding method is relatively inefficient, the implementation of mechanized precision seeding technology is a primary requirement for BC cultivation.

The term “small seeds” usually refer to seeds with an average diameter of less than 3 mm, and includes most of the seeds of vegetables and flowers [2]. BC seeds are small in size, but their regular shape and high average sphericity index are suitable for high-speed precision seeding. Precision seeding is defined as the process of using a precision seeder to make a single seed fall accurately into a reserved position in the soil according to certain agronomic requirements [3]. The seed metering device is a core component for the realization of high-speed precision seeding, and its performance is one of the most important factors that affect the quality of the seeding [4]. A pneumatic metering device has the advantages of having a low seed size requirement, does not damage the seed, is

suitable for single-grain precision seeding, and is suitable for high-speed seeding [5]. In order to meet the agronomic requirements of narrow-row dense planting of small sized seeds, and to achieve the goal of high-speed precision seeding, it is necessary to design a double-row precision metering device with a simple structure, strong adaptability, and good seeding performance [6].

At present, many experts and scholars have carried out research on pneumatic seed metering devices, but research on multi-row precision metering devices is not extensive. Research carried out has included an air-suction potato seed metering device that improved the seeding performance of large-size seed crops [7]. After theoretical analysis, the main structure and operating parameters of the device were determined. Two orthogonal tests (conventional tuber test and mini-tuber test) were then carried out to analyze the influence of the operating parameters on the seeding quality, which were then evaluated with corresponding indicators (multiple-seeding index (MTI), missing-seeding index (MI), and qualified index (QI)). The results of the conventional tuber test (mini-tuber test) indicated that the MTI was 1.1% (0.5%), MI was 0.8% (0.6%), and QI was 98.1% (98.9%) under the conditions of a 30 (35) r/min rotating speed, 25 (17) cm seed height, and 10 (3.5) kPa pickup vacuum pressure. A novel combination vacuum and spoon belt metering device to improve the efficiency and precise seeding of potatoes was designed by [8]. The structure and dimensions of the seed metering device are key components that have to be included in the experimental design to verify the seeding performance of the seed metering device. The experiment results found that, when the seeding belt speed was $0.43 \text{ m}\cdot\text{s}^{-1}$, the spoon aperture was 15.72 mm, and the cleaning air pressure was 2.94 kPa, the seeding effect of the metering device was high (the missing seed index was 3.97%, the multiple seed index was 4.65%, and the qualified seed index was 91.38%). A six-row air-blowing centralized precision seed-metering device for the realization of precision seeding of *Panax notoginseng* was designed by [9]. A mechanical model of the movement process for the seed metering device was constructed based on a method combining theoretical calculations and simulation analysis. The outlet pressure of the air nozzle and the forward velocity and cone angle of the hole were selected as the test factors for carrying out the quadratic rotation orthogonal combination test. After parameter optimization, it was found that when the cone angle of the hole was 50° , the forward velocity was less than 0.73 m/s, and the outlet pressure of the air nozzle was 0.32–0.52 kPa, the qualified index of grain spacing was higher than 94%, the miss index was less than 3%, the multiple index was less than 5%, and the coefficient of variation of the row displacement consistency was less than 5%.

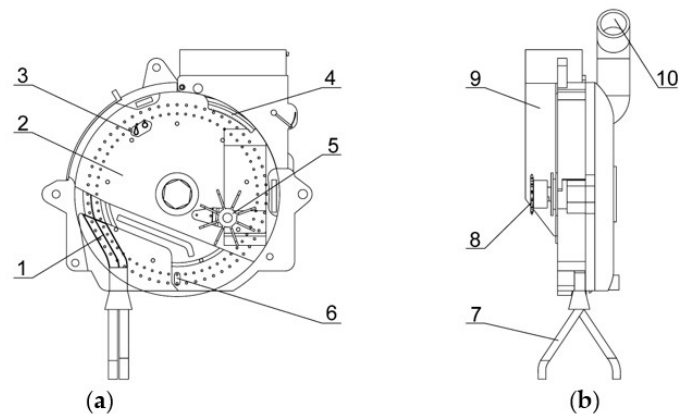
A pneumatic disk with four rows for planting rapeseed was designed by Elebaid et al. [10], and its performance under several rotating speeds and vacuum pressure values was investigated. Subsequently, the seed mass of the four-row design was measured and analyzed under the influence of rotational speed and negative pressure. It was found that the seed mass of row 1 and the seed mass of row 4 were significantly different under high-speed conditions (25 and 30 r/min). Taghinezhad et al. [11] designed and modeled a new mechanism for a sugarcane metering device with Catia software. The effect of metering device tooth length and the speed of the sugarcane billet metering device were studied in order to find the best combination for improving the distance uniformity and filling performance of the metering device cells. The analytical hierarchy process was used to select the best combination, and it was found that a 2 cm tooth length and a 0.75 m/s forward speed was the best-suited combination for the metering device, and the consistency ratio was computed as being lower than 0.1. Mandal et al. [12] designed a pneumatic seed metering mechanism for a power tiller-operated three-row precision planter. The optimum design and operating parameters of the modular seed metering device were determined by conducting experiments on the sticky belt test stand, with various performance indexes being considered. The optimum design and operation parameters were determined as follows: the number of holes for the seed metering disc was eight, the diameter of the hole was 3.5 mm, the pitch circle diameter of the disc was 116 mm, operational speed was $0.11 \text{ m}\cdot\text{s}^{-1}$, and negative pressure was 6 kPa.

The objectives of this study are to design, fabricate, and evaluate a new double-row pneumatic precision metering device for BC. Additionally, the effects of the cone angle (CA) of the suction hole, the angular velocity (AV) of the metering plate, and the negative pressure (NP) on the seeding performance of the metering device are investigated. Additionally, the range of optimal working parameters is determined and verified.

2. Materials and Methods

2.1. Structure and Working Principle of Seed Metering Device

A new double-row pneumatic precision metering device for BC was designed. The power input mechanism of the seed metering device consisted of a sprocket which transferred power to the shaft for the rotation of the metering plate. The overall structure of the seed metering device is shown in Figure 1. The seeds in the seed box become adsorbed in the suction hole of the metering plate under the effect of NP. The stirring wheel located in the seed-filling zone rotates with the metering plate under the periodic collision by the striking column. As a result, the seeds which were originally accumulated in the seed-filling zone achieved a flowing state. The seeds adsorbed by the suction hole in the seed-filling zone are transferred using the metering plate to the seed-cleaning zone. The seed cleaning devices of the inner and outer circles scrape off the multiple seeds absorbed by one hole to ensure that one seed is absorbed by one hole. The seed rotates with the metering plate to the seed-throwing zone, and due to the cut-off of the negative pressure airway, the seed breaks away from the adsorption force of NP and falls under the action of gravity and centrifugal force. The diversion channel separates the seeds from the inner and outer circles; after that, the seeds enter the diversion tube to form a double-row seed flow.



1. Diversion channel; 2. Metering plate; 3. Seed cleaning device in inner circle; 4. Seed cleaning device in outer circle; 5. Stirring wheel; 6. Anti-blocking channel; 7. Diversion tube; 8. Sprocket wheel; 9. Seed box; 10. Negative pressure outlet

Figure 1. Integral structure of seed metering device: (a) Front view; (b) Side view.

2.2. Physical Properties of *Brassica Chinensis*

“Shanghai Ai Ji” is a common variety of BC in China, and the seeds of this variety were used for the experiment. The physical properties of BC are shown in Table 1. Fifty samples were randomly selected, and the triaxial dimensions were measured using a digital vernier caliper with an accuracy of 0.01 mm. One thousand samples were weighed five times using an electronic balance with an accuracy of 0.001 g, and the mean was then calculated.

Table 1. Physical properties of *Brassica chinensis*.

Physical Properties	Maximum Value, mm	Minimum Value, mm	Mean, mm	Standard Error
Length l	2.04	1.39	1.74	0.15
Width w	1.91	1.30	1.65	0.13
Thickness h	1.97	1.33	1.63	0.16
Thousand Seed mass, g	-	-	2.410	-

According to the results of the triaxial dimensions of seeds in Table 1, the average equivalent diameter (\overline{De}) and the average spherical rate (\overline{Sp}) of the seeds can be calculated by the following formulas:

$$\overline{De} = \sqrt[3]{\bar{l} \cdot \bar{w} \cdot \bar{h}} \quad (1)$$

$$\overline{Sp} = \frac{\sqrt[3]{\bar{l} \cdot \bar{w} \cdot \bar{h}}}{\bar{l}} \times 100\% \quad (2)$$

where \bar{l} is the average length of the seeds, in mm; \bar{w} is the average width of the seeds, in mm; \bar{h} is the average thickness of the seeds, in mm; \overline{De} is the average equivalent diameter of the seeds, in mm; and \overline{Sp} is the average spherical rate of the seeds, in %.

According to the above equations, the average equivalent diameter of seeds (\overline{De}) was 1.67 mm, and the average spherical ratio (\overline{Sp}) was 96%.

2.3. Structural Design and Theoretical Analysis of the Metering Plate

2.3.1. Determination of Key Parameters for the Metering Plate

As key parts of the seed metering device, the structure parameters of the metering plate have a significant effect on seed filling performance [13,14]. The integral structure and key dimensions of the metering plate are shown in Figure 2. The position of the outer circle hole is low at the seed-filling zone, and the pressure exerted by the upper seeds on the lower seeds is large, resulting in an increase in the seed-filling resistance of the lower seeds. Moreover, the linear velocity at the center of the outer circle hole is larger than that at the inner circle hole. The seed-filling time is relatively shorter, so the outer circle hole is more difficult to fill under the same conditions. The diameter of the outer circle hole is determined according to the size of the seeds using Equation (3):

$$d_2 = (0.64 \sim 0.66)\overline{De} \quad (3)$$

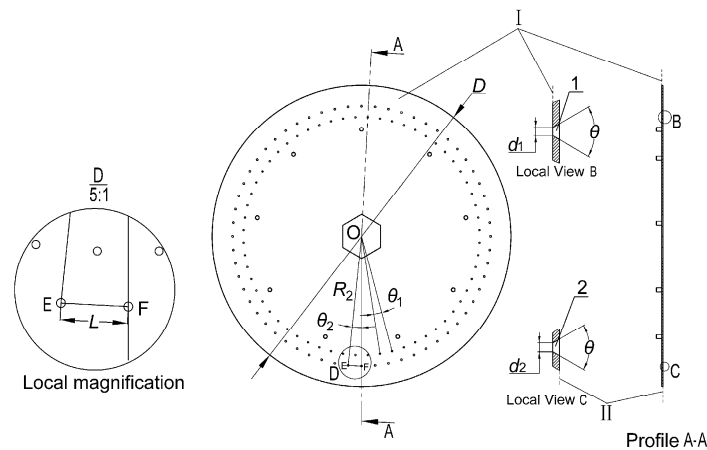
where d_2 is the diameter of the outer circle hole, in mm.

From Equation (1), the average equivalent diameter (\overline{De}) of seeds was 1.67 mm. The range of the diameter of the outer circle hole can be obtained by substituting $\overline{De} = 1.67$ mm into Equation (3): $d_2 = (1.07 \sim 1.10)$ mm. For this design, the diameter (d_2) of the outer circle hole was selected to be 1.1 mm. It is more difficult to fill the outer circle hole than the inner circle, so the diameter (d_2) of the outer circle hole was larger than the diameter (d_1) of the inner circle hole (1.0 mm).

The number of holes on the inner and outer circles determines the size of the double-row metering plate. With the increase in the number of holes of the inner and outer circles, the diameter of the metering plate increased accordingly. Similarly, the linear velocity at the center of the suction hole of the metering plate decreased. As a result, the seed-filling performance of the hole increased with the increase in the seed-filling time [15]. The number of holes was inversely proportional to the product of the rotation speed of the double-row metering plate (r/min) and the planting space of the seeds (mm), and directly proportional to the forward speed of the planter (m/s). The equation for calculating the number of holes is as follows:

$$N = \frac{60v_d}{nl} \quad (4)$$

where N is the number of holes; v_d is the forward speed of the planter, in m/s; n is the rotation speed of the double-row metering plate, in r/min; l is the planting space of the seeds, in mm.



Notes: I. The side in contact with the seed; II. The side in contact with the NP; O. The center of metering plate; E. The center of outer circle hole; F. The center of outer circle adjacent hole.

θ is the cone angle of the suction hole, °; θ_1 is the angle between two adjacent holes in the inner circle, °; θ_2 is the angle between two adjacent holes in the outer circle, °; D is the diameter of the metering plate, mm; L is the distance between point E and point F, mm; R_2 is the radius of the center of outer circle hole, mm.

Figure 2. Integral structure and key dimensions of metering plate of the seed metering device in front view and side view planes.

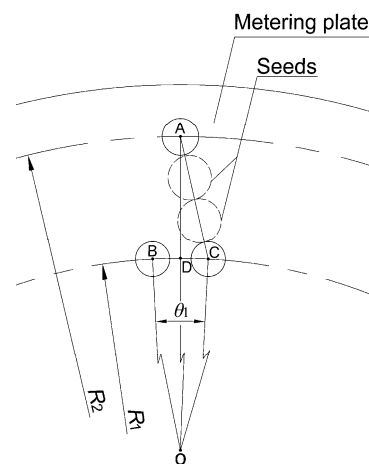
According to the agronomic requirements, the dense planting spacing of BC is 4~5 cm with a row spacing of 10~11 cm. As such, the planting space for the seeds was $l \leq 5 \text{ cm} = 0.05 \text{ m}$. According to the *Design Manual for Agricultural Machinery* [16], the linear velocity at the center of holes of the metering plate was $v \leq 0.35 \text{ m/s}$. Considering the actual installation size of the seed metering device, the radius of the metering plate with double-row holes was determined to be $R \geq 100 \text{ mm}$. According to the equation of rotation speed ($n = v/2\pi R$), it can be calculated that the rotation speed of the metering plate was $n \leq 0.557 \text{ r/s} = 33.42 \text{ r/min}$. At present, the pneumatic precision metering device can generally adapt to high-speed seeding ($v_d \geq 6 \text{ km/h} = 1.67 \text{ m/s}$). Therefore, it can be calculated from Equation (4) that $N \geq 60$, and the number of holes of the inner and outer circles was finally determined as $N_1 = N_2 = 60$.

Since the number of holes (N_1, N_2) in the inner and outer circles was 60, the angle between the two adjacent holes in the inner and outer circles is as follows: $\theta_1 = \theta_2 = 360^\circ/60 = 6^\circ$. As shown in Figure 2, three points (OEF) constitute an isosceles triangle. The distance L satisfies the following: $L > d_2 + 2l_{\max} = 1.1 \text{ mm} + 2 \times 2.04 \text{ mm} = 5.18 \text{ mm}$, where l_{\max} is the maximum length of seeds, mm. From the cosine theorem of isosceles triangle OEF, the equation for calculating R_2 is as follows:

$$R_2 = \sqrt{\frac{L^2}{2(1 - \cos(\theta_2))}} \quad (5)$$

It can be calculated from the above equation that $R_2 > 49.39 \text{ mm}$. Considering that sufficient space was reserved for the inner circle hole of the metering plate and the space of the metering plate was fully utilized, the radius of the center of the outer circle hole was determined to be 75 mm ($R_2 = 75 \text{ mm}$). The design of the metering plate diameter should be greater than $2R_2$ and a sufficient margin should be left. Combined with the *Design Manual for Agricultural Machinery* [16], the diameter of the metering plate was finally determined to be 200 mm ($D = 200 \text{ mm}$).

The space between the inner and outer circles holes is an important factor to ensure the seeding quality of a double-row metering device. Furthermore, the space of the holes directly affects the stability of seed movement. The relationship between the inner and outer holes is shown in Figure 3.



Notes: A. The center of outer circle hole; B. The center of inner circle hole; C. The center of inner circle adjacent hole; D. The center of arc length BC; O. The center of the metering plate

Figure 3. Geometry relationship of holes of inner and outer circles.

According to Figure 3, the following geometric relationships are determined:

$$\begin{cases} \text{Pythagorean theorem : } l_{AD}^2 + l_{CD}^2 = l_{AC}^2 \\ \text{Restrictions on length AC : } l_{AC} > \frac{d_1 + d_2}{2} + 2\overline{De} \end{cases} \quad (6)$$

$$\begin{cases} l_{CD} = R_1 \sin\left(\frac{\theta_1}{2}\right) \\ R_1 = R_2 - l_{AD} \end{cases} \quad (7)$$

where R_1 is the radius of the center of the inner circle hole, in mm.

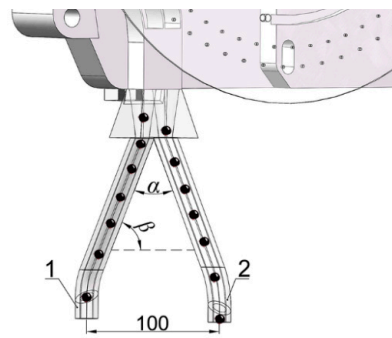
The spacing (l_{AD}) between the inner and outer holes can be obtained from Equations (6) and (7):

$$l_{AD} > \sqrt{\left(\frac{d_1 + d_2}{2} + 2\overline{De}\right)^2 - \left[\left(R_2 - l_{AD}\right) \sin\left(\frac{\theta_1}{2}\right)\right]^2} \quad (8)$$

The spacing between the inner and outer holes can be obtained ($l_{AD} > 2.18$ mm) by substituting the known parameters into Equation (8). Taking into account the reasonable use of the space of the metering plate and the non-interference of the inner and outer holes, the spacing between the holes of the inner and outer circles (l_{AD}) was determined to be 8 mm.

2.3.2. Design of Diversion Tube for Seed Metering Device

The diversion tube guides the seeds placed on the metering plate of double-row holes to form double-rows and the seeds flow and fall smoothly along the surface of the wall. The seeds drop from the outer circle holes through the No. 1 diversion tube, and the inner circle holes through the No. 2 diversion tube. The diversion tube is shown in Figure 4.



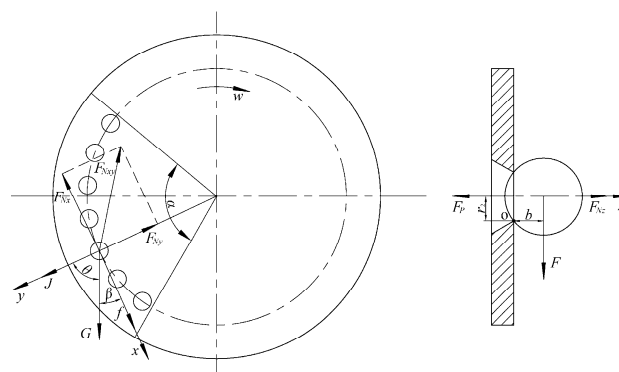
α is the diversion angle, °; β is the angle between diversion tube and horizontal plane, °.

Figure 4. The structure of diversion tube.

After analyzing the process of seed-dropping, the diversion angle α of the diversion tube was finally determined to be 60° . According to the experiment measurements, the static friction coefficient was completed earlier and the average value of the static friction angle between the seed and the diversion tube (Material: DSM IMAGE8000) was 18.95° . When β is greater than the static friction angle, the relative movement occur between the solid surfaces. The angle β can be calculated as: $\beta = (180^\circ - \alpha)/2 = 60^\circ$. The seeds can fall smoothly in the diversion tube and form double-row seed flows at $\beta > 18.95^\circ$. In this study, narrow rows were considered for planting BC, and row space was set to 100 mm (10 cm) according to agronomic requirements.

2.3.3. Force Analysis of Seed-Filling Process

Owing to high average spherical ratio, the seeds of BC can be regarded as a sphere during the force analysis of the seed-filling process. The force analysis is aimed at the outer circle seeds that are difficult to be adsorbed by the suction hole in the seed-filling zone. During the seed-filling process, the force acting on the adsorbed seeds was divided into component forces in three directions (x, y, z), as shown in Figure 5.



Note: f is the friction resistance of air and seed population to adsorbed seed, N; G is gravity, N; J is the centrifugal force of the seed; F_{Nx} is the support of the suction hole to the seed in the x axis direction, N; F_{Ny} is the support of the suction hole to the seed in the y axis direction, N; F_{Nz} is the support of the suction hole to the seed in the z axis direction, N; F_{Nxy} is the resultant force of F_{Nx} and F_{Ny} , N; F_P is the adsorption force on the seed, N; F is the resultant force of J , G , and f , N; α is the seed-filling zone; β is the angle between G and x axis, °; θ is the angle between G and y axis, °; b is the distance between F and o , m; r_2 is the distance between F_P and o , m;

Figure 5. Force analysis of seeds on suction holes.

A suction hole adsorbs a single seed, which must meet the following moment equilibrium conditions:

$$F_b \leq F_P r_2 \quad (9)$$

For the seeds to be steadily adsorbed by the suction hole, the equilibrium condition of forces must be satisfied in the xy plane:

$$\begin{cases} x \text{ axis : } f + G \cos(\beta) = F_{Nx} \\ y \text{ axis : } J + G \cos(\theta) = F_{Ny} \end{cases} \quad (10)$$

The resultant force F_{Nxy} of F_{Nx} and F_{Ny} on the xy plane are obtained according to Equation (10):

$$F_{Nxy} = \sqrt{F_{Nx}^2 + F_{Ny}^2} = \sqrt{(f + G \cos(\beta))^2 + (J + G \cos(\theta))^2} \quad (11)$$

Since F is numerically equal to F_{Nxy} ($F = F_{Nxy}$), Equation (9) is rewritten as follows:

$$F_P \geq \frac{\sqrt{(f + G \cos(\beta))^2 + (J + G \cos(\theta))^2} b}{r_2} \quad (12)$$

According to the pressure formula ($P = F/S$), the adsorption pressure of the suction hole is as follows:

$$\begin{aligned} P = \frac{F_P}{S} &\geq \frac{\sqrt{(f + G \cos(\beta))^2 + (J + G \cos(\theta))^2} b}{r_2 S} \\ &\geq \frac{\sqrt{(f + G \cos(\beta))^2 + (J + G \cos(\theta))^2} b}{\pi r_2^2} \end{aligned} \quad (13)$$

where P is the adsorption pressure of the suction hole, in Pa; S is the area of suction hole, in mm^2 ; $f = mg\lambda$, $\lambda = (6\sim 10)\tan(\varepsilon)$, ε is the angle of repose of seeds, in $^\circ$; $J = mv^2/R_2$, v_h is the linear velocity at the center of the suction hole, in m/s.

The 1000-grain weight of the seed measured in the early stage was 2.41 g, so the average mass of each seed was 2.41×10^{-6} kg ($m = 2.41 \times 10^{-6}$ kg). The angle $\theta = 60^\circ$ and $\beta = 30^\circ$ were measured when the hole was at the optimum seed-filling position. In the early stage, the angle of repose of seeds was measured to be 25.46° ($\varepsilon = 25.46^\circ$), so the value of λ can be calculated as 3.809 ($\lambda = 8 \tan(25.46^\circ) = 3.809$). According to the *Design Manual for Agricultural Machinery* [16], the linear velocity at the center of the holes of the metering plate was $v \leq 0.35$ m/s. The range of distance b was determined to be 1.21–1.83 mm, so the average value of b was 1.52 mm ($b = 0.00152$ m). Substituting the above parameters into Equation (13), the P obtained is greater than 324.4 Pa ($P \geq 324.4$ Pa).

2.4. Experimental Materials and Equipment

The seeds of "Shanghai Ai Ji" were used as experimental material for the study. A self-built double-row metering device bench (Figure 6) was used for the experiments.



1. Conveyor belt; 2. Digital display governor; 3. Vacuum tube; 4. Bench; 5. Piezometric tube; 6. Positive pressure tube

Figure 6. Experimental object and devices: (a) Seeds of "Shanghai Ai Ji"; (b) Experimental devices used for seeding performance.

2.5. Experimental Methods and Evaluation Indicators

Combined with the research results of relevant scholars and previous experimental research, the main parameters affecting seeding performance were determined to be negative pressure, angular velocity of the metering plate, and cone angle of the suction hole. Therefore, NP, AV, and CA were selected as the main experimental factors of this experiment [17,18].

A suitable NP value can adsorb the seeds and ensure that only one seed is adsorbed by one suction hole. According to the theoretical calculation results, the minimum value of NP was ($P \geq 324.4$ Pa) and based on the design of this study, a combination of a double-row metering plate coupled with the existence of pressure loss resulted in the selection requirements for the NP value being relatively strict [19]. After the pre-experiment, the NP value was selected to be 0.5~2.5 kPa. It was found that when the rotation speed of the metering plate exceeded 35 r/min (converted to AV of 3.67 rad/s), the seeding performance of the metering device decreased sharply. As such, the AV of the metering plate was changed at 1.5–3.5 rad/s. The change in the CA of the suction hole directly affected the change in the flow field at the suction hole, which led to a change in adsorption force of the suction hole. According to the pre-experiment, when the CA of the suction hole changed from 45° to 75°, it was observed that the adsorption situation of the suction hole of the inner and outer circles was good. Therefore, three kinds of metering plate with different cone angles of the suction hole were custom-machined, having cone angles of 45°, 60°, and 75°.

Each group of experiments was repeated three times, and its average value was taken. According to the National Standard of P.R.C (GB/T 6973-2005 Testing Methods of Single Seed Drills (Precision Drills)) [20], the QI and the MI of the inner and outer circles of the metering device were determined as the indexes of seeding performance in this experiment. This experiment measured 180 samples of planting spacing. The dense planting spacing of BC was 4~5 cm according to the agronomic requirements, so the theoretically qualified planting spacing (L) of this experiment was set to 4.5 cm. According to the requirements where the planting spacing was within the range of ($0.5L = 2.25$ cm, and $1.5L = 6.75$ cm), it was qualified spacing; where the planting spacing was greater than 6.75 cm, it was miss spacing; and where the planting spacing was less than 2.25 cm, it was multiple spacing. Qualified spacing and miss spacing coupled with the total sample number (180) were used to calculate the qualified index (QI) and miss index (MI), respectively, as percentages. The experimental scheme is shown in Table 2.

Table 2. Experiment factors and levels.

Level	NP ^[a] x_1 , kPa	AV ^[b] x_2 , rad·s ⁻¹	CA ^[c] x_3 , °
−1	0.5	1.5	45
0	1.5	2.5	60
1	2.5	3.5	75

Note: ^[a] NP = Negative pressure; ^[b] AV = Angular velocity; ^[c] CA = Cone angle.

3. Results and Discussion

3.1. Single Factor Experiment

3.1.1. Effect of Negative Pressure on Seeding Performance

From Figure 7, it can be seen that when the AV of the metering plate was 2.5 rad/s and the CA was 60°, the influence trend of NP on the seeding performance of the inner and outer circles was essentially similar. With increase in NP, the QI of the inner and outer circles first increased and then decreased, and the MI of the inner and outer circles decreased continuously. The qualified index of the outer circle (Q_O) reached the maximum value ($Q_{Omax} = 95.45\%$) and the qualified index of the inner circle (Q_I) reached the maximum value ($Q_{Imax} = 94.58\%$) when the NP was 1.71 and 1.63 kPa, respectively.

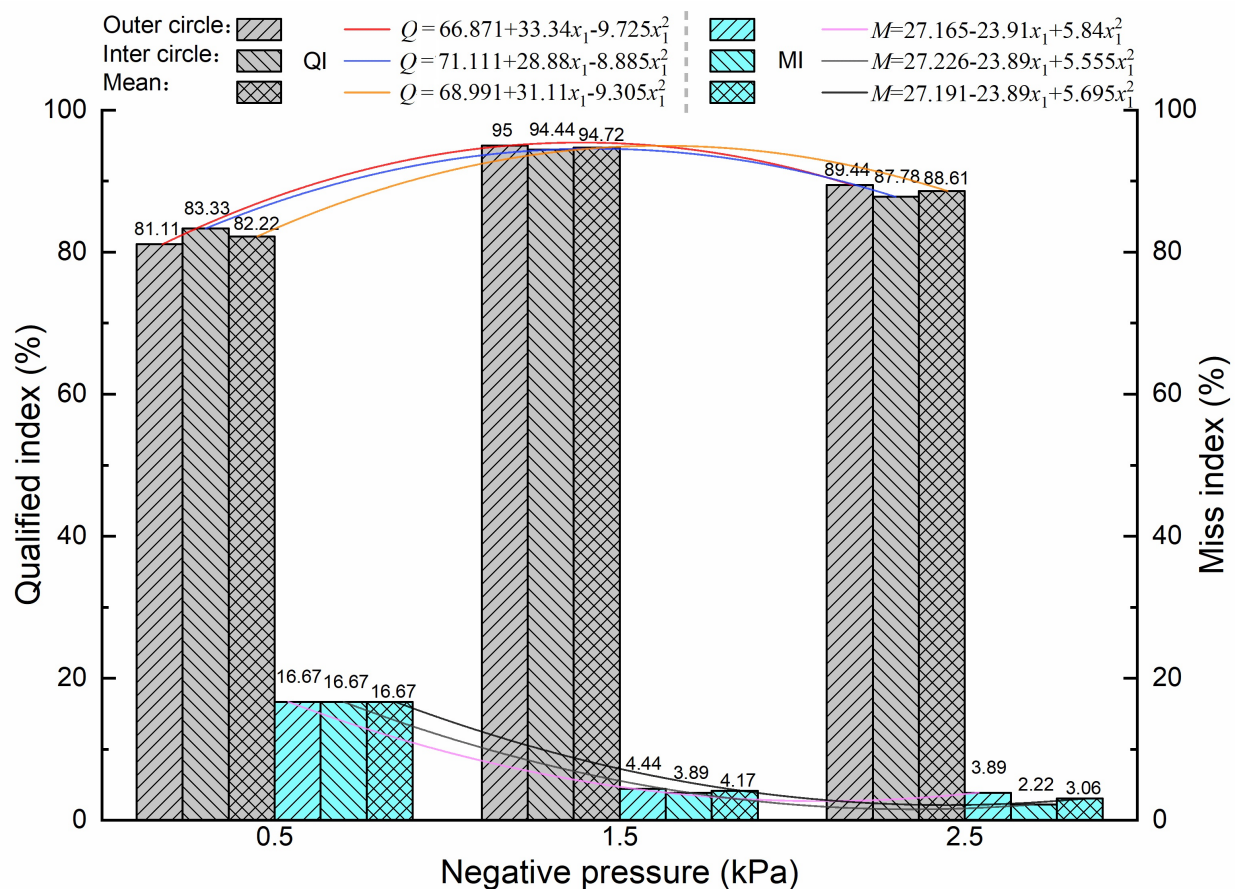


Figure 7. Effect of NP on seeding performance at AV of 2.5 rad/s and CA of 60°.

When the NP value was low, the adsorption force of the suction holes on the seeds was relatively small such that the phenomenon of missed suctioning occurred in the suction hole of the inner and outer circles. This resulted in the MI being high ($M \geq 7\%$). At this time, owing to the large radius of the outer circle, the high linear velocity at the center of the suction hole of the outer circle, and the smaller time of seed-filling, the Q_I was higher than the Q_O . When the NP gradually increased, the adsorption force of the suction holes on the seeds also increased, and the MI of the inner and outer circles decreased sharply. When the NP was too high, there were some suction holes in the inner and outer circles that adsorbed multiple seeds, which led to an increase in the multiple index of the inner and outer circles. As a result, the QI was reduced at this time.

From Figure 7, it can also be seen that the QI of inner and outer circles was high ($Q \geq 92\%$) and the MI of inner and outer circles was low ($M \leq 4\%$) when the NP was in the range of 1.57–2.16 kPa.

3.1.2. Effect of Angular Velocity on Seeding Performance

The influence trend of AV of the metering plate on the seeding performance of the inner and outer circles was fundamentally similar (Figure 8) at 1.5 kPa negative pressure and 60° cone angle.

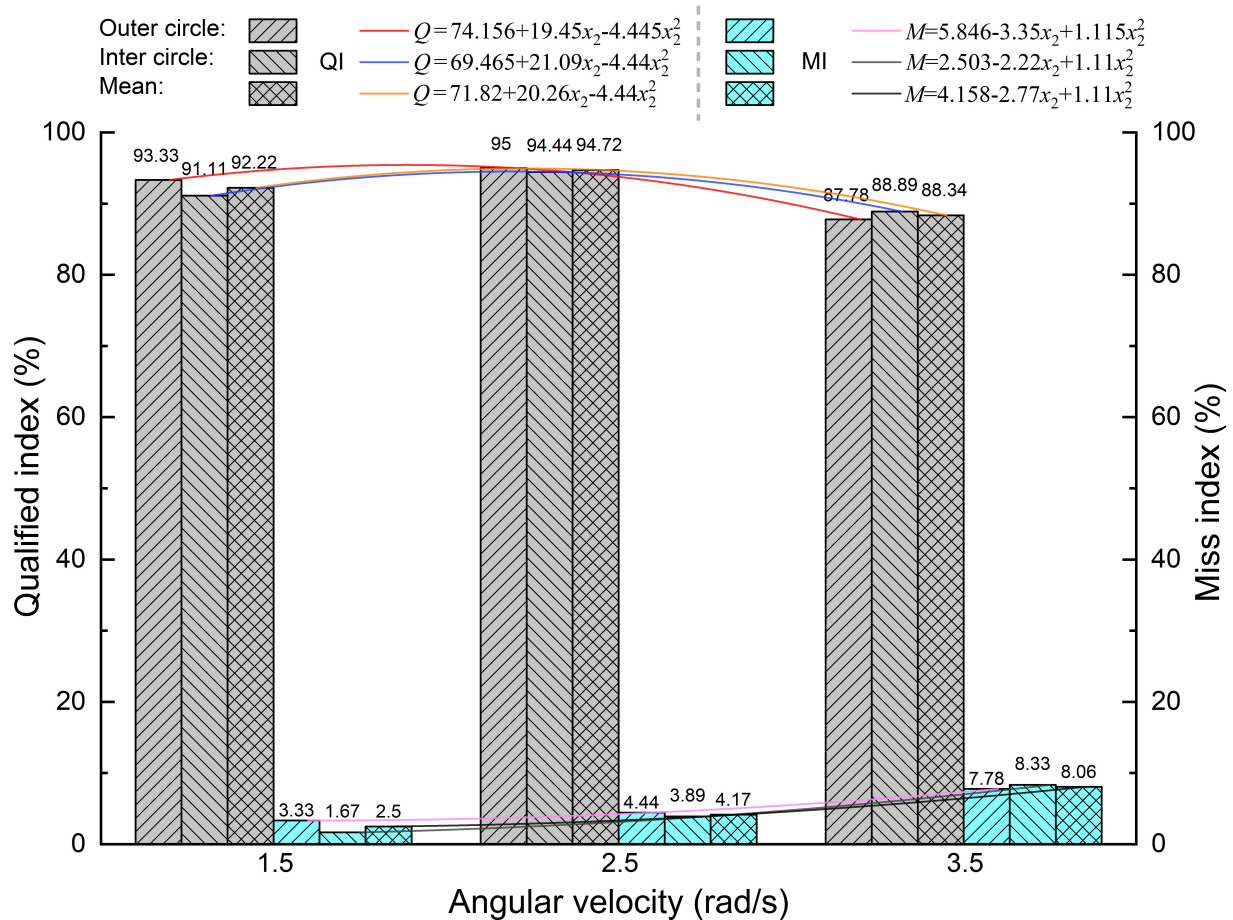


Figure 8. Effect of AV on seeding performance at NP of 1.5 kPa and CA of 60°.

When the AV of the metering plate was low, the seed cleaning device of the inner circle had weaker collision strength for the seeds which then were reabsorbed by the suction hole. As a result, there was a higher multiple index for the inner circle, such that the Q_O was higher than the Q_I . When the AV of the metering plate gradually increased, the QI of inner and outer circles first increased and reached the peak ($Q_{I\max} = 94.58\%$, $Q_{O\max} = 95.45\%$), and then decreased. Where the AV of the metering plate was too large, the seed-filling time of the suction hole was too short when the metering plate passed through the seed-filling zone. As a result, there was missed suctioning of the suction hole of the inner and outer circles, so that the MI of the inner and outer circles was high ($M \geq 7\%$).

From Figure 8, it can also be seen that the QI of the inner and outer circles was high ($Q \geq 92\%$) and the MI of the inner and outer circles was low ($M \leq 4\%$) when the AV was in the range of 1.62–2.28 rad/s.

3.1.3. Effect of Cone Angle on Seeding Performance

The influence trend of CA of the suction hole on the seeding performance of the inner and outer circles was fundamentally similar (Figure 9) at 1.5 kPa negative pressure and 2.5 rad/s angular velocity.

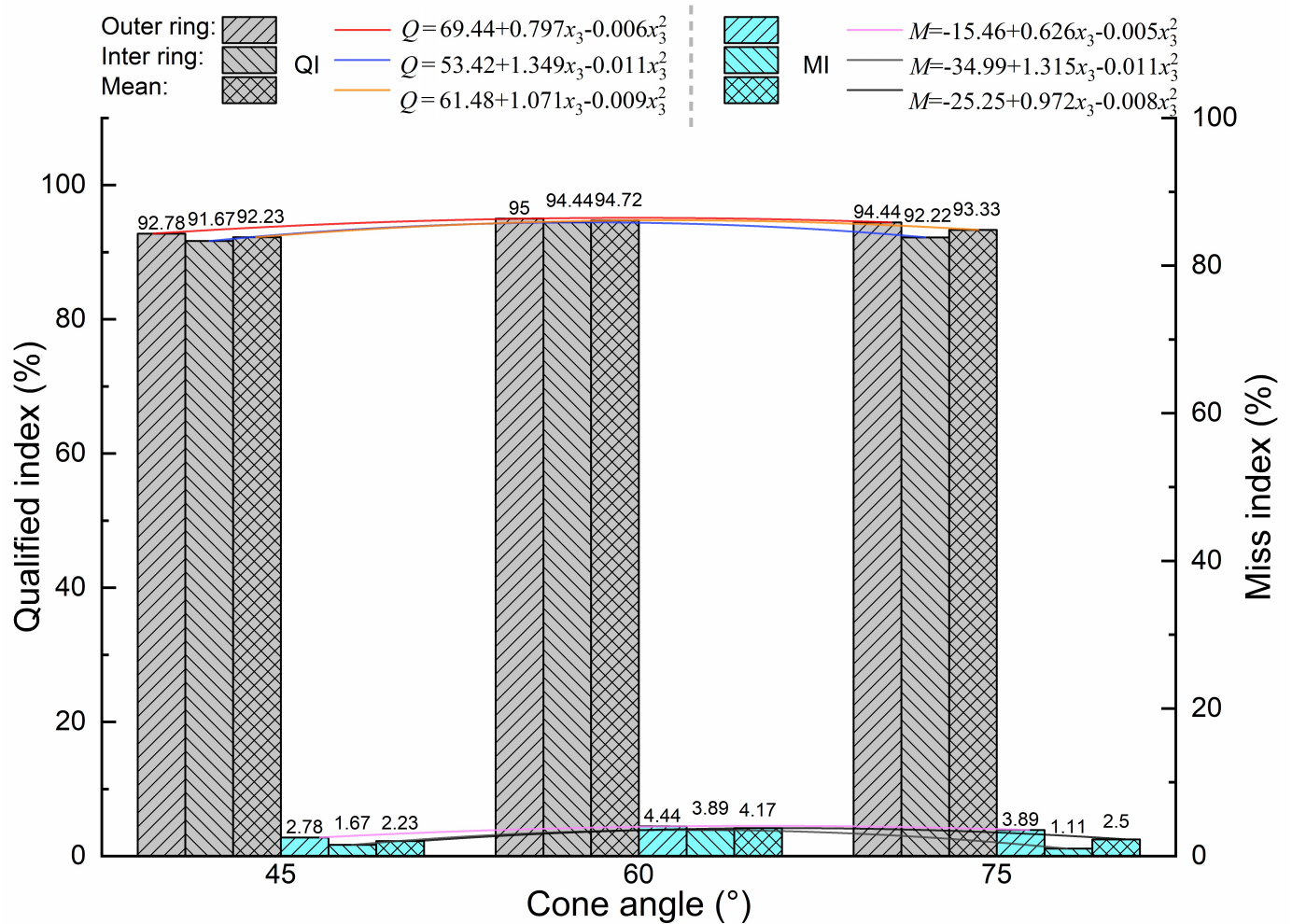


Figure 9. Effect of CA on seeding performance at NP of 1.5 kPa and AV of 2.5 rad/s.

When the CA of the suction hole was small, the adsorption force of the suction hole acting on the seed was relatively concentrated, which led to the phenomenon of some suction holes in the inner and outer circles adsorbing multiple seeds, so that the QI of the inner and outer circles was not high ($Q \leq 93\%$). When the CA of the suction hole increased, the QI of the inner and outer circles first increased and reached the peak ($Q_{I\max} = 94.78\%$, $Q_{O\max} = 95.91\%$), and then decreased.

3.2. Central Composite Design Experiment

3.2.1. Experimental Design and Results

The experimental scheme design and coding of influencing factors was performed according to the Central Composite Design in Design-Expert 8.0.6 software. This software was also used to process and analyze the experimental data. The experiment scheme and results are shown in Table 3.

Table 3. Experimental scheme and results.

NO.	NP ^[a] x_1 , kPa	AV ^[b] x_2 , rad·s ⁻¹	CA ^[c] x_3 , °	QI ^[d] , %	MI ^[e] , %	QI, %	MI, %
				OC ^[f]		IC ^[g]	
1	-1	-1	-1	85.56	13.33	91.11	8.33
2	1	-1	-1	92.78	3.33	88.89	2.22
3	-1	1	-1	78.33	21.67	74.44	25.56
4	1	1	-1	91.11	4.44	88.33	6.11
5	-1	-1	1	87.22	9.44	91.67	7.22
6	1	-1	1	92.78	3.89	87.78	1.67
7	-1	1	1	77.22	22.78	75.00	25.00
8	1	1	1	92.22	4.44	87.22	3.33
9	-1	0	0	81.11	16.67	83.33	16.67
10	1	0	0	89.44	3.89	87.78	2.22
11	0	-1	0	93.33	3.33	91.11	1.67
12	0	1	0	87.78	7.78	88.89	8.33
13	0	0	-1	92.78	2.78	91.67	1.67
14	0	0	1	94.44	3.89	92.22	1.11
15	0	0	0	95.00	4.44	94.44	3.89
16	0	0	0	92.78	3.33	93.33	2.78
17	0	0	0	93.33	5.00	92.78	4.44
18	0	0	0	92.78	4.44	91.67	3.89
19	0	0	0	94.44	3.89	94.44	3.33
20	0	0	0	93.89	4.44	92.78	3.89

Note: ^[a] NP = Negative pressure; ^[b] AV = Angular velocity; ^[c] CA = Cone angle; ^[d] QI = Qualified index; ^[e] MI = Miss index; ^[f] OC = Outer circle; ^[g] IC = Inner circle.

3.2.2. Analysis of Variance

Multiple regression fitting of the experimental results was performed using ANOVA in Design-Expert 8.0.6 software. This is shown in Table 4. After multiple regression analysis, the regression equations of the QI (Q) of the inner and outer circles, the MI (M) of the inner and outer circles, and various influencing factors can be obtained as follows:

$$Q_O = 101.399 + 19.622x_1 + 1.951x_2 - 0.893x_3 + 1.875x_1x_2 + 0.005x_1x_3 - 0.014x_2x_3 - 6.567x_1^2 - 1.287x_2^2 + 0.008x_3^2 \quad (14)$$

$$M_O = 10.811 - 19.610x_1 - 1.740x_2 + 0.397x_3 - 2.503x_1x_2 + 0.028x_1x_3 + 0.037x_2x_3 + 5.935x_1^2 + 1.210x_2^2 - 0.004x_3^2 \quad (15)$$

$$Q_I = 93.042 + 12.154x_1 - 1.755x_2 - 0.151x_3 + 4.028x_1x_2 - 0.028x_1x_3 + 1.591 \times 10^{-15}x_2x_3 - 6.036x_1^2 - 1.591x_2^2 + 0.002x_3^2 \quad (16)$$

$$M_I = -15.778 - 15.550x_1 + 1.872x_2 + 0.961x_3 - 3.683x_1x_2 - 0.014x_1x_3 - 0.014x_2x_3 + 6.288x_1^2 + 1.843x_2^2 - 0.008x_3^2 \quad (17)$$

From Table 4, it can be seen that the P -value of each evaluation indicator (Q_O , M_O , Q_I , M_I) is less than 0.01, indicating that the regression model established in this paper is highly significant. Furthermore, the lack of fit for each model was greater than 0.05, which indicates that the four regression equations are highly fitted. The coefficients of determination (R^2) of the four models are 0.965, 0.990, 0.947, and 0.991, respectively. These coefficients of determination are all close to 1, indicating that the four models had a high fitting degree to the experimental data. The non-significant factors with p -value > 0.05 were eliminated according to the significant level p -value of different influencing factors in each model, and the following optimized regression equations were obtained:

$$Q_O = 84.880 + 19.036x_1 - 5.314x_2 + 1.875x_1x_2 - 6.278x_1^2 \quad (18)$$

$$M_O = 15.121 - 16.804x_1 + 2.373x_2 - 2.503x_1x_2 + 5.557x_1^2 + 0.832x_2^2 \quad (19)$$

$$Q_I = 97.688 + 12.710x_1 - 9.709x_2 + 4.028x_1x_2 - 6.778x_1^2 \quad (20)$$

$$M_I = 9.248 - 14.478x_1 + 4.202x_2 - 3.683x_1x_2 + 5.654x_1^2 + 1.209x_2^2 - 0.0003x_3^2 \quad (21)$$

Table 4. ANOVA for response surface quadratic model.

EI ^[a]	Source	SS ^[b]	DF ^[c]	F Value	p-Value	Significance
Q_O ^[d]	Model	538.09	9	30.60	<0.0001	**
	x_1 -NP	239.02	1	122.33	<0.0001	**
	x_2 -AV	62.55	1	32.01	0.0002	**
	x_3 -CA	1.10	1	0.56	0.4699	
	x_1x_2	28.13	1	14.39	0.0035	**
	x_1x_3	0.04	1	0.02	0.8902	
	x_2x_3	0.34	1	0.18	0.6835	
	x_1^2	118.59	1	60.69	<0.0001	**
	x_2^2	4.55	1	2.33	0.1578	
	x_3^2	8.60	1	4.40	0.0623	
	Residual	19.54	10			
	Lack of Fit	15.44	5	3.76	0.0861	
	Pure Error	4.10	5			
	Cor Total	557.63	19			
M_O ^[e]	Model	728.02	9	109.13	<0.0001	**
	x_1 -NP	408.32	1	550.86	<0.0001	**
	x_2 -AV	77.23	1	104.19	<0.0001	**
	x_3 -CA	0.12	1	0.17	0.6921	
	x_1x_2	50.10	1	67.59	<0.0001	**
	x_1x_3	1.39	1	1.88	0.2002	
	x_2x_3	2.46	1	3.32	0.0982	
	x_1^2	96.88	1	130.70	<0.0001	**
	x_2^2	4.03	1	5.44	0.0419	*
	x_3^2	2.80	1	3.78	0.0805	
	Residual	7.41	10			
	Lack of Fit	5.77	5	3.50	0.0976	
	Pure Error	1.65	5			
	Cor Total	735.44	19			
Q_I ^[f]	Model	562.37	9	19.84	<0.0001	**
	x_1 -NP	59.78	1	18.98	0.0014	**
	x_2 -AV	134.54	1	42.71	<0.0001	**
	x_3 -CA	0.03	1	0.01	0.9239	
	x_1x_2	129.77	1	41.19	<0.0001	**
	x_1x_3	1.39	1	0.44	0.5209	
	x_2x_3	1.14E-13	1	3.61E-14	1.0000	
	x_1^2	100.19	1	31.80	0.0002	**
	x_2^2	6.96	1	2.21	0.1680	
	x_3^2	0.34	1	0.11	0.7476	
	Residual	31.50	10			
	Lack of Fit	25.73	5	4.45	0.0634	
	Pure Error	5.78	5			
	Cor Total	593.87	19			
M_I ^[g]	Model	1000.81	9	120.17	<0.0001	**
	x_1 -NP	451.99	1	488.43	<0.0001	**
	x_2 -AV	222.97	1	240.95	<0.0001	**
	x_3 -CA	3.09	1	3.34	0.0975	
	x_1x_2	108.49	1	117.23	<0.0001	**
	x_1x_3	0.34	1	0.37	0.5554	
	x_2x_3	0.35	1	0.38	0.5507	
	x_1^2	108.72	1	117.49	<0.0001	**
	x_2^2	9.34	1	10.09	0.0099	**
	x_3^2	8.59	1	9.28	0.0123	*
	Residual	9.25	10			
	Lack of Fit	7.61	5	4.65	0.0586	
	Pure Error	1.64	5			
	Cor Total	1010.07	19			

Note: ^[a] EI = Evaluation Indicators; ^[b] SS = Sum of Squares; ^[c] DF = Degree of Freedom; ^[d] Q_O = Qualified index of outer circle; ^[e] M_O = Miss index of outer circle; ^[f] Q_I = Qualified index of inner circle; ^[g] M_I = Miss index of inner circle; * (0.01 < p < 0.05); ** (p < 0.01).

It can be seen from Equations (18)–(21) that the significant factors that affect the Q_I of the inner and outer circles are NP (x_1), AV (x_2), the interaction term of NP and AV (x_1x_2), and the quadratic term of NP (x_1^2). The significant factors affecting the MI of the inner and

outer circles are NP (x_1), AV (x_2), the interaction term of NP and AV (x_1x_2), the quadratic term of NP (x_1^2), and the quadratic term of AV (x_2^2). In addition to the above, other factors affecting the miss index of the inner circle (M_I) include quadratic term of the CA (x_3^2).

3.2.3. Effect of Interaction Factors on Seeding Performance

The descending dimension method was used to adjust the coding of any of the three influencing factors of NP, AV, and CA to zero [21], and the response surface diagram of the interaction of the other two influencing factors on the seeding performance of the inner and outer circle was plotted, as shown in Figures 10 and 11.

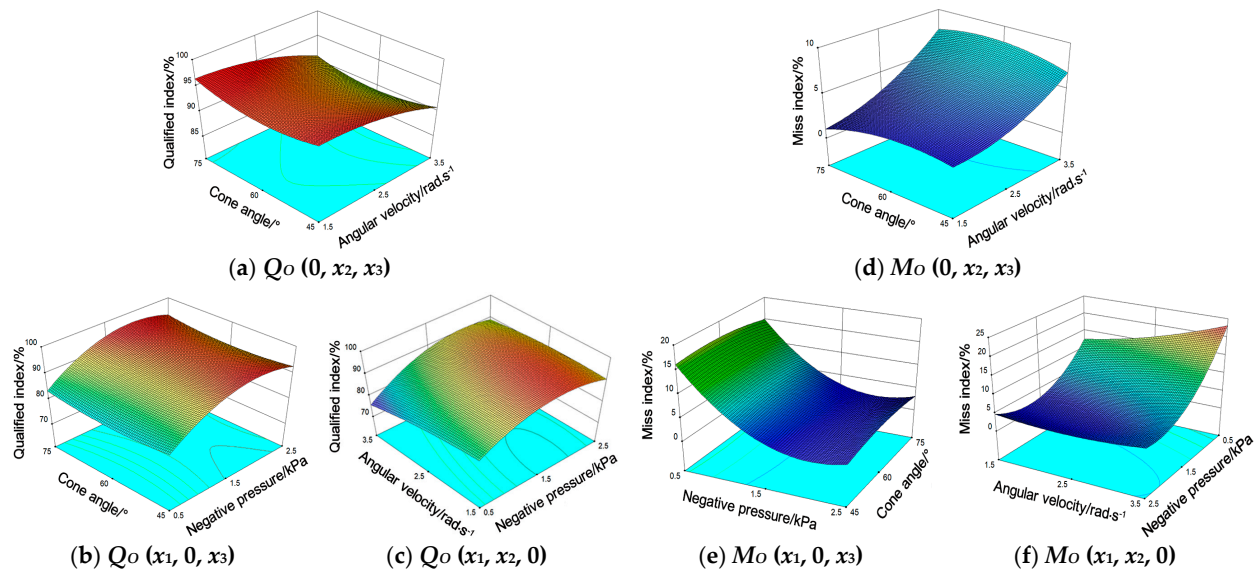


Figure 10. Effect of interaction factors on seeding performance of outer circle when NP = 1.5 kPa, AV = 2.5 rad/s, and CA = 60°, respectively

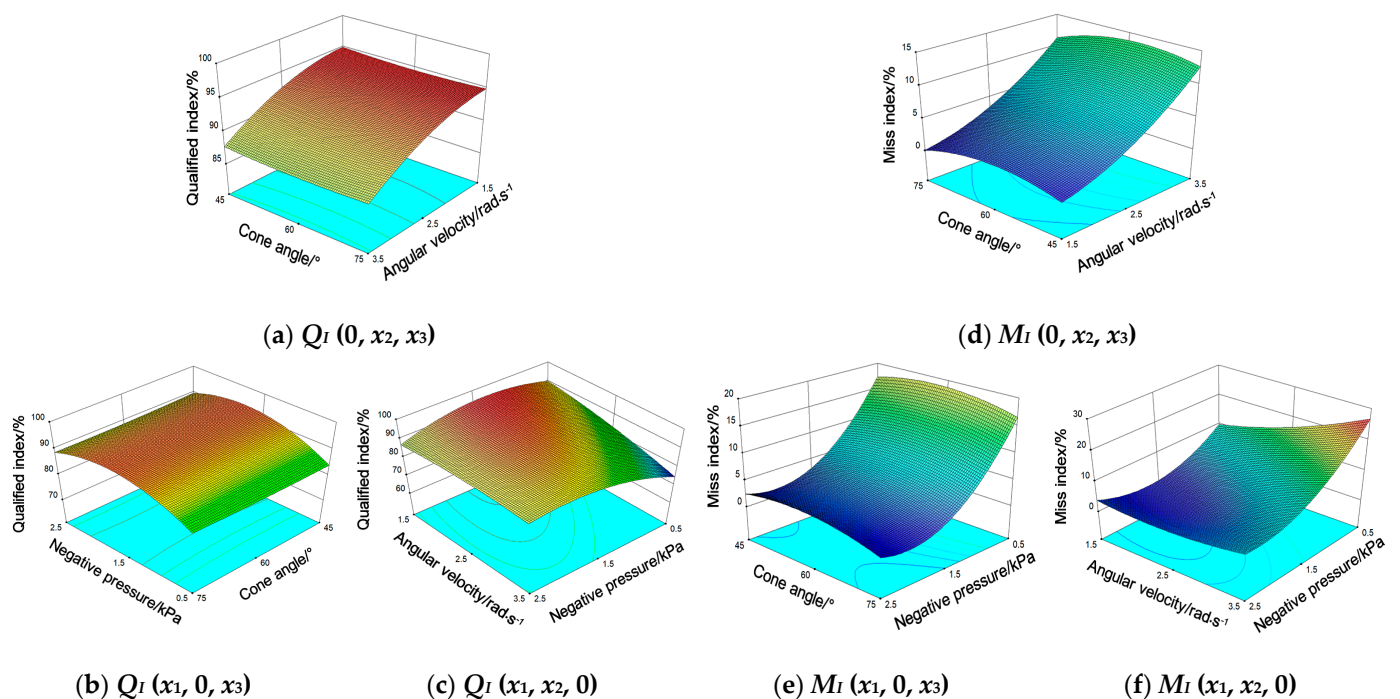


Figure 11. Effect of interaction factors on seeding performance of inner circle when NP = 1.5 kPa, AV = 2.5 rad/s, and CA = 60°, respectively.

It can be seen from Figure 10a at 1.5 kPa negative pressure under similar CA, the Q_O decreased with an increase in AV, but the trend for M_O was the opposite. This can be attributed to the shortening of the residence time of the metering plate in the seed-filling zone with the increase in the AV of the metering plate, resulting in missed suctioning of the suction hole. Under the condition of similar AV, the change in CA had no significant effect on the Q_O and M_O .

Figure 10b shows that when the AV of the metering plate was 2.5 rad/s, under the condition of similar CA, the Q_O increased with the increase in NP, and then decreased, while the M_O was the opposite. At 0.5–1.8 kPa negative pressure, the suction force of the holes for seeds gradually increased with the increase in NP, so that the QI increased significantly and the MI decreased suddenly. When the NP was in the range of 1.8–2.5 kPa, one suction hole adsorbed multiple seeds because of the excessive adsorption force, which led to an increase in multiple index and decrease in QI. Under the condition of similar NP, the change in CA had no significant effect on the Q_O and M_O .

It can be seen from Figure 10c that when the CA was 60° , under the condition of similar AV, the Q_O first increased and then decreased with the increase in NP, while the M_O was completely opposite. Under the condition of similar NP, the Q_O first increased and then decreased with the increase in AV. When the AV was in the range of 1.5–2.2 rad/s, the residence time of the metering plate in the seed-filling zone was lengthy, and this was beneficial to the suction hole for seed-filling, since it increased the Q_O . When the AV was greater than 2.2 rad/s, the residence time of the metering plate in the seed-filling zone was shortened, and the phenomenon of missed suctioning of the suction hole increased. As a result, the M_O increased rapidly.

Figure 11a shows that when the NP was 1.5 kPa, under the condition of similar AV, the change in CA had no significant effect on the Q_I , while the M_I first increased and then decreased with the increase in CA. Under the condition of similar CA, Q_I decreased with the increase in AV, but the trend for M_I was the opposite. It can be seen from Figure 11b that when the AV of the metering plate was 2.5 rad/s, under the condition of similar NP, the change in CA had no significant effect on the Q_I and M_I . Under the condition of similar CA, when the NP was in the range of 0.5–1.7 kPa, Q_I increased with the increase in NP, but the M_I decreased sharply with the increase in NP. When NP was greater than 1.7 kPa, Q_I decreased with the increase in NP. From Figure 11c, it is evident that when CA was 60° , under the condition of similar AV, the Q_I first increased and then decreased with the increase in NP, while the trend for M_O was the opposite. When the NP was low ($NP \leq 1.4$ kPa), the effect of AV on the Q_I and M_I was significant. Q_I decreased with the increase in AV, while the trend for M_I was the opposite. When NP was large ($NP > 1.4$ kPa), the effect of AV on Q_I and M_I was not significant. Overall, it was determined from the figure that Q_I was high ($Q_I > 92\%$) and M_I was low ($M_I < 5.5\%$) when NP was in the range of 1.2–1.6 kPa and AV was in the range of 1.65–2.35 rad/s.

3.2.4. Parameter Optimization

In order to explore the optimal parameter combination, the parameter optimization design was carried out. According to the National Standard of P.R.C (GB/T 6973-2005 Testing Methods of Single Seed Drills (Precision Drills)) [20], under the premise of ensuring a high QI and low MI of seeding, parameter optimization was carried out with the goal that the QI of the inner and outer circle was greater than 94% and the MI was less than 2.5%. This is shown in Figure 12. According to the previous single factor experiment on CA, when the other two factors were at zero level and CA was 60° , the performance of

seeding was better. There, CA was set at 60° . The parameter optimization conditions are as follows:

$$\left\{ \begin{array}{l} 94\% \leq (Q_O(x_1, x_2, x_3), Q_I(x_1, x_2, x_3)) \leq 100\% \\ 0 \leq (M_O(x_1, x_2, x_3), M_I(x_1, x_2, x_3)) \leq 2.5\% \\ \text{s.t.} \left\{ \begin{array}{l} 0.5 \text{ kPa} \leq x_1 \leq 2.5 \text{ kPa} \\ 1.5 \text{ rad/s} \leq x_2 \leq 3.5 \text{ rad/s} \\ x_3 = 60^\circ \end{array} \right. \end{array} \right. \quad (22)$$

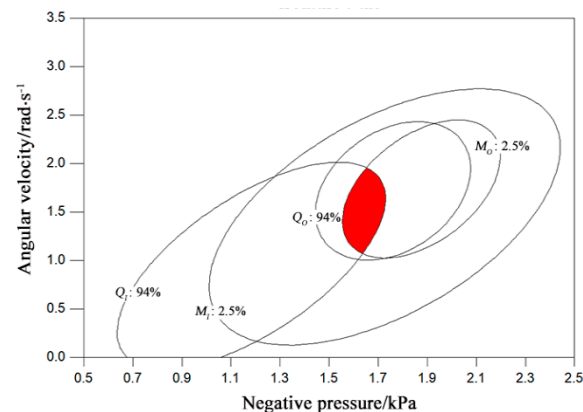


Figure 12. Parameter optimization area.

The graph intersection area is the parameter optimization area as described in Figure 12. When NP was 1.55–1.72 kPa and AV was 1.1–1.9 rad/s, the seeding performance was excellent.

3.2.5. Bench Verification Experiment

A bench verification experiment was used to verify whether the expected seeding performance [$94\% \leq (Q_O, Q_I) \leq 100\%$, $0 \leq (M_O, M_I) \leq 2.5\%$] and excellent CV of the seed mass could be achieved under the condition of optimized parameters, and the experiment was repeated three times and five times, respectively, under the median value of the range of parameter optimization (NP = 1.63 kPa, AV = 1.5 rad/s, CA = 60°). The results of the bench verification experiments are shown in Tables 5 and 6. It was observed from the experiment results that the seeding performance was excellent ($(Q_O, Q_I) > 94\%$, $(M_O, M_I) < 2.5\%$) and CV was good (CV of the seed mass in the outer and inner circle: 5.15%; CV of total seed mass: 8.60%) under the condition of optimized parameters. Therefore, the parameter optimization results were accurate.

Table 5. The results of seeding performance.

Experiment Indices		Number of Experiments			Mean	Standard Error
		NO.1	NO.2	NO.3		
QI, %	OC	94.58	94.17	95.42	94.72	0.52
	IC	94.17	94.58	94.58	94.44	0.19
MI, %	OC	2.08	2.5	2.5	2.36	0.20
	IC	2.08	1.25	1.67	1.67	0.34

Table 6. The results of coefficient of variation of seed mass.

Experiment Indices	Number of Experiments					Mean	TSM ^[a]	RE ^[b] , %	CV ^[c] , %	CV of Total Seed Mass, %
	NO.1	NO.2	NO.3	NO.4	NO.5					
Seed mass of outer circle, g	1.838	1.808	1.769	1.824	1.816	1.811	2.068	12.43	5.15	8.60
Seed mass of inner circle, g	2.072	1.897	1.972	1.910	1.889	1.948	2.068	5.80		
Total seed mass, g	3.910	3.705	3.741	3.734	3.705	3.759	4.136	9.12		

^[a] TSM = Theoretical seed mass; ^[b] RE = Relative error; ^[c] CV = Coefficient of variation.

4. Conclusions

1. Aiming at the characteristics of small size and high sphericity of BC seeds and meeting the row spacing of seeding by agronomic requirements, a double-row pneumatic metering device that can be used for high-speed and precise double-row seeding was developed. The metering device can complete double-row seeding with a double-row metering plate, and can meet different row spacing of seeding requirements by replacing different diversion tubes. Furthermore, the structure and key dimensions of the double-row metering plate were determined, the other key components of metering device were designed, and the force analysis of the seed-filling process was carried out.
2. The NP, the AV of the metering plate, and the CA of the suction hole were selected as the main influencing factors of the experiment. A single factor experiment was carried out to investigate the influence of each factor on the seeding performance of the inner and outer circles.
3. For further exploring the relationship between the seeding performance and the NP, AV, and CA, the CCD scheme was applied in the experiment. Moreover, the experimental results were analyzed by ANOVA, and the regression equation between the evaluation indicators and the influencing factors was established. It was found from ANOVA that the NP, AV, the interaction term of NP and AV, the quadratic term of NP, the quadratic term of AV, and the quadratic term of CA were significant factors affecting the seeding performance of the inner and outer circles. Furthermore, the effect of interaction factors on the seeding performance of the inner and outer circle was also studied.
4. To explore the best combination of parameters, the parameters were optimized with the goal that the QI of the inner and outer circle was greater than 94% and the MI was less than 2.5%. After parameter optimization, it was found that when the NP was 1.55–1.72 kPa, the AV was 1.1–1.9 rad/s, and the CA was 60°, the seeding performance of the metering device and the coefficient of variation (CV) of the seed mass were good.

Author Contributions: Conceptualization, B.L., H.L. and X.Q.; methodology, B.L. and R.A.; software, B.L. and S.M.N.; validation, B.L., J.W. and S.L.; formal analysis, B.L. and X.C.; investigation, B.L. and H.L.; resources, B.L. and R.A.; data curation, B.L.; writing—original draft preparation, B.L.; writing—review and editing, B.L., H.L., X.Q., R.A., S.M.N., J.W., X.C. and S.L.; supervision, H.L. and X.Q.; project administration, H.L.; funding acquisition, J.W. All authors have read and agreed to the published version of the manuscript.

Funding: This research was supported by the National Key R&D Program of China “Vegetable Intelligent Fine Production Technology and Equipment R&D” (Grant No. 2017YFD0701302).

Data Availability Statement: The data presented in this study are available on request from the corresponding author. The data are not publicly available due to privacy.

Acknowledgments: We would like to thank “College of Engineering, Nanjing Agricultural University” and “College of Mechanical and Power Engineering, Nanjing Tech University”.

Conflicts of Interest: The authors declare no conflict of interest.

Abbreviations

NP	Negative pressure (kPa)
AV	Angular velocity (rad/s)
CA	Cone angle (°)
CCD	Central composite design
ANOVA	Analysis of variance
QI	Qualified index (%)
MI	Miss index (%)
CV	Coefficient of variation (%)
BC	<i>Brassica chinensis</i>
MTI	Multiple index (%)
Q _O	Qualified index of outer circle (%)
Q _I	Qualified index of inner circle (%)
OC	Outer circle
IC	Inner circle

References

- Han, W.; Sun, C.X.; Zhao, H.L.; Hu, Q.; Zheng, Q.Z.; Song, X.L. Compensatory Ability and Defense Mechanism of Chinese Cabbage under High Temperature Stress. *Chin. J. Agrometeorol.* **2018**, *39*, 119–128. [\[CrossRef\]](#)
- Jin, X.; Li, Q.W.; Zhao, K.X.; Zhao, B.; He, Z.T.; Qiu, Z.M. Development and test of an electric precision seeder for small-size vegetable seeds. *Int. J. Agric. Biol. Eng.* **2019**, *12*, 75–81. [\[CrossRef\]](#)
- Singh, R.C.; Singh, G.; Saraswat, D.C. Optimisation of Design and Operational Parameters of a Pneumatic Seed Metering Device for Planting Cottonseeds. *Biosyst. Eng.* **2005**, *92*, 429–438. [\[CrossRef\]](#)
- Yang, L.; Yan, B.X.; Cui, T.; Yu, Y.M.; He, X.T.; Liu, Q.W.; Liang, Z.J.; Yin, X.W.; Zhang, D.X. Global overview of research progress and development of precision maize planters. *Int. J. Agric. Biol. Eng.* **2016**, *9*, 9–26. [\[CrossRef\]](#)
- Chen, J.; Li, Y.M.; Wang, X.Q.; Zhao, Z. Finite Element Analysis for the Sucking Nozzle Air Field of Air-suction Seeder. *Trans. Chin. Soc. Agric. Mach.* **2007**, *9*, 59–62.
- Li, Y.H.; Yang, L.; Zhang, D.X.; Cui, T.; Ding, L.; Wei, Y.N. Design and Experiment of Pneumatic Precision Seed-metering Device with Single Seed-metering Plate for Double-row. *Trans. Chin. Soc. Agric. Mach.* **2019**, *50*, 61–73. [\[CrossRef\]](#)
- Lü, J.Q.; Yang, Y.; Li, Z.H.; Shang, Q.Q.; Li, J.C.; Liu, Z.Y. Design and experiment of an air-suction potato seed metering device. *Int. J. Agric. Biol. Eng.* **2016**, *9*, 33–42. [\[CrossRef\]](#)
- Zhang, W.Z.; Liu, C.L.; Lv, Z.Q.; Qi, L.; Lv, H.Y.; Hou, J.L. Optimized Design and Experiment on Novel Combination Vacuum and Spoon Belt Metering Device for Potato Planters. *Math. Probl. Eng.* **2020**, *2020*, 1–12. [\[CrossRef\]](#)
- Lai, Q.H.; Sun, K.; Yu, Q.Y.; Qin, W. Design and experiment of a six-row air-blowing centralized precision seed-metering device for *Panax notoginseng*. *Int. J. Agric. Biol. Eng.* **2020**, *13*, 111–122. [\[CrossRef\]](#)
- Elebaid, J.I.; Liao, Q.X.; Wang, L.; Liao, Y.T.; Yao, L. Design and experiment of multi-row pneumatic precision metering device for rapeseed. *Int. J. Agric. Biol. Eng.* **2018**, *11*, 116–123. [\[CrossRef\]](#)
- Taghinezhad, J.; Alimardani, R.; Jafari, A. Development and Evaluation of a New Mechanism for Sugarcane Metering Device Using Analytical Hierarchy Method and Response Surface Methodology. *Sugar Tech* **2015**, *17*, 258–265. [\[CrossRef\]](#)
- Mandal, S.; Kumar, G.V.P.; Tanna, H.; Kumar, A. Design and Evaluation of a Pneumatic Metering Mechanism for Power Tiller Operated Precision Planter. *Curr. Sci.* **2018**, *115*, 1106. [\[CrossRef\]](#)
- Yan, B.X.; Zhang, D.X.; Cui, T.; He, X.T.; Ding, Y.Q.; Yang, L. Design of pneumatic maize precision seed-metering device with synchronous rotating seed plate and vacuum chamber. *Trans. Chin. Soc. Agric. Eng.* **2017**, *33*, 15–23. [\[CrossRef\]](#)
- Jia, H.L.; Zhang, S.W.; Chen, T.Y.; Zhao, J.L.; Guo, M.Z.; Yuan, H.F. Design and Experiment of Self-suction Precision Mung-bean Metering Device. *Trans. Chin. Soc. Agric. Mach.* **2020**, *51*, 51–60. [\[CrossRef\]](#)
- Cheng, X.P.; Lu, C.Y.; Meng, Z.J.; Yu, J.Y. Design and parameter optimization on wheat precision seed meter with combination of pneumatic and type hole. *Trans. Chin. Soc. Agric. Eng.* **2018**, *34*, 1–9. [\[CrossRef\]](#)
- Chinese Academy of Agricultural Mechanization Sciences. *Design Manual for Agricultural Machinery*; China Agricultural Science and Technology Press: Beijing, China, 2007; Volume 1, pp. 343–368.
- Zhai, J.B.; Xia, J.F.; Zhou, Y. Design and Experiment of Pneumatic Precision Hill-drop Drilling Seed Metering Device for Hybrid Rice. *Trans. Chin. Soc. Agric. Mach.* **2016**, *47*, 75–82. [\[CrossRef\]](#)
- Shi, L.R.; Sun, B.G.; Zhao, W.Y.; Yang, X.P.; Xin, S.L.; Wang, J.X. Optimization and Test of Performance Parameters of Elastic Air Suction Type Corn Roller Seed-metering Device. *Trans. Chin. Soc. Agric. Mach.* **2019**, *50*, 88–95, 207. [\[CrossRef\]](#)
- Chen, M.Z.; Diao, P.S.; Zhang, Y.P.; Gao, Q.M.; Yang, Z.; Yao, W.Y. Design of pneumatic seed-metering device with single seed-metering plate for double-row in soybean narrow-row-dense-planting seeder. *Trans. Chin. Soc. Agric. Eng.* **2018**, *34*, 8–16. [\[CrossRef\]](#)

-
20. National Standards of the P.R.C National Standard of the People's Republic of China. *GB/T 6973-2005: Testing Methods of Single Seed Drills (Precision Drills)*; Standardization Administration of the P.R.C: Beijing, China, 2005.
 21. Chen, H.T.; Li, T.H.; Wang, H.F.; Wang, Y.; Wang, X. Design and parameter optimization of pneumatic cylinder ridge three-row close-planting seed-metering device for soybean. *Trans. Chin. Soc. Agric. Eng.* **2018**, *34*, 16–24. [[CrossRef](#)]